The Indonesian Journal of Computer Science
www.ijcs.net
Volume 14, Issue 2, April 2025
https://doi.org/10.33022/ijcs.v14i2.4798

Nonlinear Analysis of Seismic Vulnerability in Mass Irregular Reinforced Concrete Buildings

Aeint Myet Chawe[1], Nang Su Le'. Mya Thwin[2]
aeintmyetchawe.tu@gmail.com[1], nangsule.myathwin@gmail.com[2]
[1]Ph.D candidate, Department of Civil Engineering, Mandalay Technological University
[2]Professor, Department of Civil Engineering, Mandalay Technological University

Article Information

Received : 15 Mar 2025
Revised : 21 Apr 2025
Accepted : 30 Apr 2025

Keywords

ETABS, Fragility Curves, Mass irregularity, Pushover analysis, Seismic vulnerability index

Abstract

With Myanmar's growing population, buildings adapt through architectural and functional irregularities. However, such irregular structures are more susceptible to earthquake damage than regular ones. This study develops a vulnerability index for a 143-ft, 12-story reinforced concrete condominium building with mass irregularities in Mandalay, designed per ASCE/MNBC seismic codes. Mass irregularity is considered at three locations in the same condominium reinforced concrete building: the lower, middle, and upper thirds. By evaluating these three locations, the study investigates how the position of mass irregularity influences a building's seismic vulnerability in pushover (nonlinear) analysis. Guidelines provided by the HAZUS-MH MR4 technical manual have been used to develop fragility curves. Based on the study analyzing the structural vulnerability of irregular frame buildings by plotting fragility curves and determining a vulnerability index based on plastic hinge formation, the VI values of bottom mass, middle mass, and top mass building were 0.71, 0.00, and 0.94 respectively. It appears that the maximum vulnerability index value is observed in the top mass irregular building. Among all irregular buildings, the top mass irregular building was found to be more vulnerable, and the middle mass irregular building was found to perform better than others.

A. Introduction

The seismic behaviour of a structure is determined by several factors, including stiffness, lateral strength, ductility, vertical and plan configuration [1]. Buildings with vertical irregularities are among the most common types of irregular structures, primarily due to functional and architectural demands. Modern multi-story designs increasingly incorporate reinforced concrete structures with vertical irregularities for both serviceability and aesthetic purposes. However, these structures tend to be highly vulnerable during earthquakes. In contrast, regular buildings maintain a uniform distribution of mass, stiffness, strength, and structural form. When any of these properties—alone or in combination—are unevenly distributed in any direction, the structure is classified as irregular [2]. Numerous studies have been conducted to assess the structural vulnerability of irregular reinforced concrete buildings, often utilizing fragility curves to estimate the likelihood of damage under a given seismic hazard. In the Mandalay area, which comprises six townships, is one of the largest urban areas in Myanmar. In line with continuous development and progress, the population is growing steadily. Therefore, to meet the needs of this growing population, the demand for building structures is increasing. Currently in Mandalay, urban building construction systems have incorporated irregularity into regular buildings, both from an architectural standpoint. However, these buildings may need to withstand large earthquakes in the future; therefore their behavior and vulnerability when subjected to earthquakes need to be evaluated. In preliminary seismic risk assessment, there are several parameters considered such as the soil type, seismic zoning, structural system, material type, height, irregularities, and etc. Among these parameters, irregularity types are most commonly found in the buildings that are actually being constructed in Mandalay. Several researchers investigated the influence of the magnitudes and locations of vertical irregularities on the seismic response of the buildings[3]. Building on this foundation, the primary objective of this study is to examine the impact of mass irregularity location. To achieve this, an existing 12-story, rectangular-shaped reinforced concrete building in the densely populated Aung Myay Thar Zan township of Mandalay was selected for analysis. According to MNBC 2020 [4] and ASCE 7-16 [5], the selected building is classified as mass irregular at various locations. To analyze the structure, twelve three-dimensional reinforced concrete moment-resisting frames were modeled and analyzed using the finite element software ETABS [6], employing nonlinear static (pushover) analysis. The results from this analysis were utilized to generate fragility curves and assess the probability of structural damage. The HAZUS MH-MR4 technical manual [7] was used for generating the fragility curve. Additionally, vulnerability index values were calculated based on plastic hinge formation from the pushover analysis. These values were then used to evaluate the seismic vulnerability of the irregular buildings under consideration.

B. Research Method

Geometric and Model Descriptions

The structure considered in this study is based on an existing twelve-story condominium building in Mandalay, which features a reinforced concrete frame structural system. Three different locations of mass irregularities were considered for the same building: (a) bottom mass model (i.e., bottom one-third of the building with heavy mass), (b) middle mass model (i.e., middle one-third of the building with heavy mass), (c) top mass model (i.e., top one-third of the building with heavy mass). The plan view and the 3D structural model are shown in Figure 1 and mass irregularity building models are shown in Figure 2. The length of one span in the shorter X-direction is 73 ft, and in the longer Y-direction, it is 164 ft. The first story height is 12 ft, the other typical story height is 11 ft, and the stair roof story height is 10 ft, which makes the total height of the building, 143 ft. All ground floor vertical elements are fixed at the bottom level of the structure, and the site is characterized by soft clay soil, classified as site class "E." A thickness of 4.5 in for slabs in membrane-type buildings is quite common for all structural models. The compressive strength of concrete, f_c', 4000 psi, and the yield strength of reinforcing bars, f_y, 50000 psi are considered for all structural elements. The corresponding modulus of elasticity, E_c , amounts to 3600 ksi and the steel elastic modulus, E_s , is 29×10^3 ksi. Floors were considered as rigid diaphragms. The applied loads and load combinations were referred according to MNBC 2020 [4] and ASCE 7-16 [5]. The self-weight of the building elements is automatically computed using ETABS software [6]. The ratios of Poission, μ , for concrete and steel are equal to 0.2 and 0.3, respectively and the building structural elements were initially designed in accordance with ACI 318-19 [8]. The description of mass irregularities and design results for all structural elements are tabulated in Table 1.

Table 1. Irregularities Description and Design Results (for all models)

Symbol	Model	Irregularity Position	Magnitude of Irregularity	Column Size (in. × in.)	Beam Size (in. × in.)
BMI	Bottom mass irregularity	1-4	500%	40 × 20	15 × 24
				30 × 30	15 × 21
				36 × 18	15 × 18
				27 × 27	12 × 18
				18 × 18	12 × 15
				15 × 15	10 × 15
				12 × 12	10 × 12
MMI	Middle mass irregularity	5-8	500%	40 × 20	15 × 24
				30 × 30	15 × 21
				36 × 18	15 × 18
				27 × 27	12 × 18
				18 × 18	12 × 15
				15 × 15	10 × 15
				12 × 12	10 × 12
TMI	Top mass irregularity	9-12	500%	40 × 20	15 × 24
				30 × 30	15 × 21
				36 × 18	15 × 18
				27 × 27	12 × 18
				18 × 18	12 × 15
				15 × 15	10 × 15
				12 × 12	10 × 12

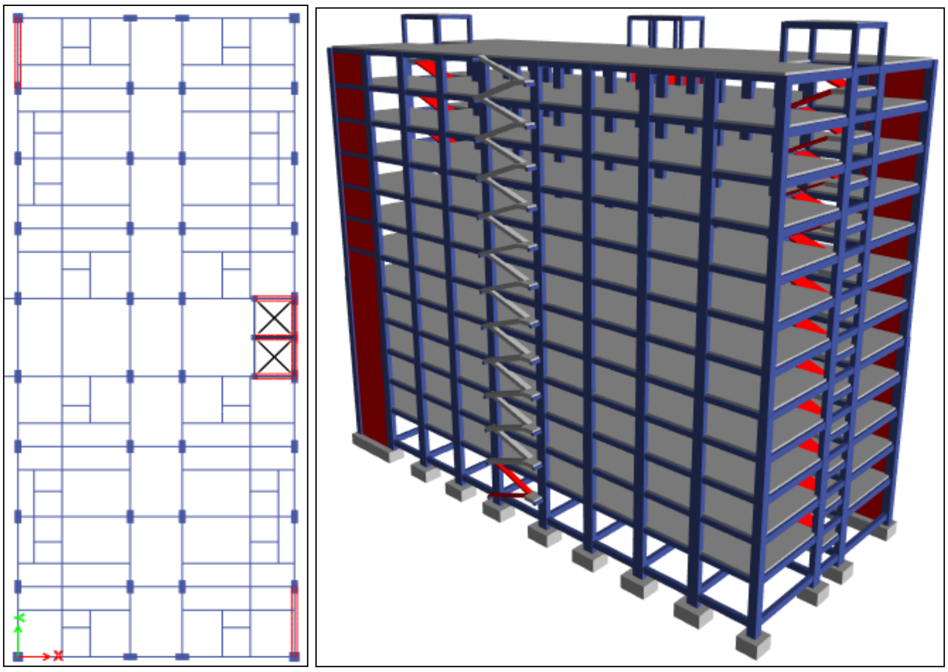

Figure 1. Building Plan (left); 3D Structural Model (right)

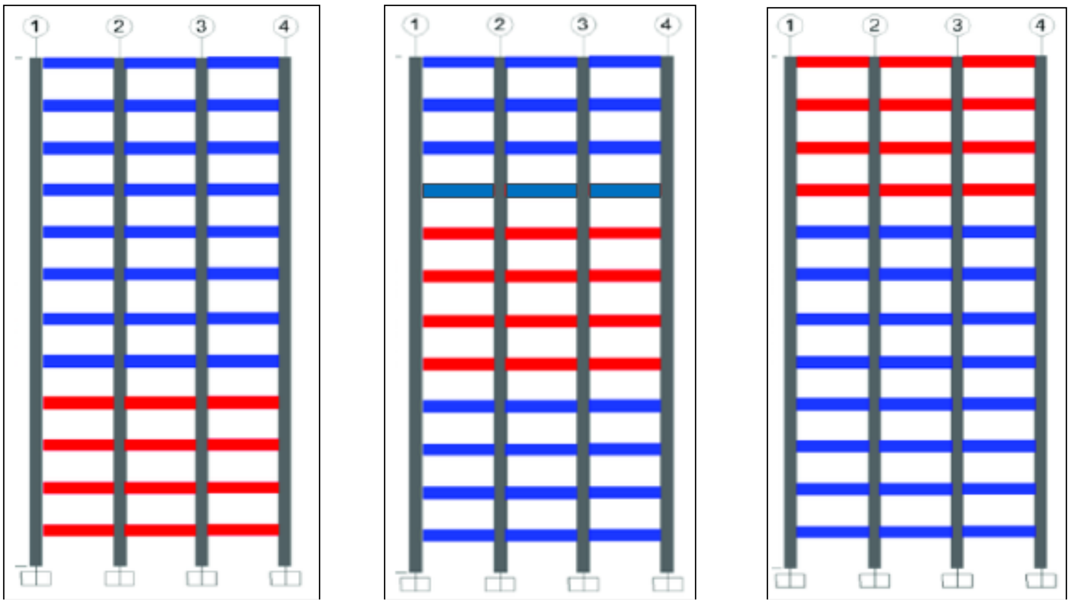

(a) **(b)** **(c)**

Figure 2. Mass Irregularity Building Models: (a) bottom mass irregularity (b) middle mass irregularity (c) top mass irregularity

Pushover Analysis of Structure

A nonlinear static pushover analysis was performed in ETABS, utilizing default hinges. M3 hinges were assigned to beam ends, while P-M2-M3 hinges were applied to column ends, in accordance with ASCE 41-17 [9] recommendations. The model was pushed to a target displacement, which was determined by 4% of the height of the structure as per ATC-40 [10] guidelines. This target displacement represents the building's expected displacement during the design earthquake.

The P-Δ effect has been incorporated by considering the geometric non-linearity parameter. For seismic vulnerability assessment, the pushover curves in the X and Y directions are converted into ARDS (Acceleration Displacement Response Spectrum) format as per FEMA440 [11]. The obtained capacity curves are bilinearized to determine the yield spectral displacement, S_{dy} and ultimate spectral displacement values, S_{du}. These yield and ultimate spectral displacement values are used to obtain median values at different damage states. The values of medians at different damage states are obtained from damage state model proposed by Lantada*et al* [12] are shown in Table 2.

Table 2. Damage State Thresholds [12]

Dmage States	Median Value of Spectral Displacement, S_{ds}
Slight	$0.7\ S_{dy}$
Moderate	S_{dy}
Extensive	$S_{dy} + 0.25\ (S_{du} - S_{dy})$
Complete	S_{du}

Generation of Fragility Curves

Damage state Betas, β_{ds}, shown in Table 3, for each building height category are selected from the 'Building Fragility Betas' table in the HAZUS MH-MR4 technical manual [7]. These include slight, moderate, extensive, and complete damage states. In this study, spectral displacement is used to quantify ground motion severity.

Table 3. Damage State Beta Values [7]

Dmage States	Damage State Beta "β_{ds}"		
	Low-rise building	Mid-rise building	High-rise building
Slight	0.81	0.68	0.66
Moderate	0.84	0.67	0.64
Extensive	0.86	0.68	0.67
Complete	0.81	0.81	0.78

Fragility curves are developed for both the longitudinal X and transverse Y directions across different building models. The probability of reaching or exceeding a given damage state is represented by a cumulative lognormal distribution. For structural damage states, the probability of being in or exceeding a specific damage state ds , given the spectral displacement, S_d , is defined by equation (1):

$$P\ [\ ds/S_d] = \Phi\ [\ 1/\ \beta_{ds} \ln(\ S_d/\ S_{d,ds})] \qquad (1)$$

Where $S_{d,ds}$ is the median spectral displacement at which the building reaches the damage state threshold ds, β_{ds} is the standard deviation of the natural logarithm of spectral displacement for damage state ds, and Φ represents the standard normal cumulative distribution function. $P[S/S_d]$, $P[M/S_d]$, $P[E/S_d]$, $P[C/S_d]$ indicate probability of being in or exceeding slight (S), moderate (M), extensive (E) and complete (C), respectively. In this study, seismic demands, including spectral displacement and spectral acceleration, are used for generating the fragility curves.

Vulnerability Index

Vulnerability index is an estimation of the damage caused to the structure after the structure has been pushed to its target displacement. In other words, this index is calculated after performing nonlinear static analysis. It is a linear combination of the various hinges formed in the member along with a weightage factor assigned to each hinge state as shown in equation (2). The hinge status of each individual member constituting the structure with respect to the prefixed objective displacement is taken into account in calculating the vulnerability index. These hinges are considered either at the performance point of the structure or at the point where the analysis will be terminated. However, in this study, the hinge status equivalent to the collapse prevention state of the structure has been considered. Modifying the building vulnerability index proposed by Lakshmanan [13] to create a local vulnerability index for the frames of each story is a significant step towards assessing the seismic vulnerability of individual structural elements within a building. The modified equation for the local vulnerability index for the frame of each story, based on Lakshmanan's original building vulnerability index is expressed as follows:

$$VI_{Loc_i} = \frac{[1.5\Sigma N_j^c\ x_j + \Sigma N_j^h\ x_j]_i}{[\Sigma N_j^c + \Sigma N_j^h]_i} \qquad (2)$$

Where $N_J{}^C$ and $N_J{}^h$ are the number of hinges in columns and beams, respectively, for the j^{th} performance range. The summation sign covers the performance ranges j=1,2,3,4,5,6. The i indicates the story frames under consideration. Assessing the states of plastic hinges in structural members is crucial for understanding the potential interactions among elements within the structure, especially during seismic events. The ATC-40 [10] hinge recommendations are given in Table 4.

Table 4. Vulnerability Index Weightage Factors [13]

Serial Number	Performance Range (j)	Weightage Factor (x_j)
1	< B	0
2	B-IO	0.125
3	IO-LS	0.375
4	LS-CP	0.625
5	CP-C	0.875
6	C-D, D-E, and > E	1.000

C. Result and Discussion

This study introduces an analytical approach to developing fragility curves for existing reinforced concrete building in the Mandalay area, with a particular focus on Aung Myay Thar Zan Township. The probability of failure is assessed based on the seismic response. Fragility curves depict the probability of exceeding a particular damage state as a function of the seismic demand (such as peak ground acceleration, spectral displacement, or intensity measure). The X-axis typically represents the seismic intensity (e.g., peak ground acceleration). The Y-axis represents the probability of exceeding a certain damage state. Each curve corresponds to a specific damage state (slight, moderate, extensive, or collapse). The curve starts from zero and rise as the seismic intensity increases. The slope of the curve reflects the structure's sensitivity to damage at varying intensities. When carrying out non-linear static analysis, the results offer insights into the behavior of a structure or system under applied loads, considering non-linearities in material properties, geometry, and boundary conditions. The probability of failure is assessed based on the seismic response, and fragility curves are developed for mass irregular reinforced concrete buildings. Table 5 and Table 6 show the failure probabilities of the bottom mass irregular building at different damage states for the push X and Y directions, respectively. The corresponding fragility curves are presented in Figure 3 and Figure 4.

Table 5. Probabilities of Failures for Bottom Mass Irregular Building (Push X direction)

S_d (in)	Probability of Failures (%)			
	Slight	Moderate	Extensive	Complete
0	0	0	0	0
0.1	4	1	0	0
0.2	24	10	4	1
0.3	47	26	12	3
0.4	64	42	23	7
0.5	76	56	34	11
0.6	83	67	44	16
0.7	89	75	53	21
0.8	92	81	61	27
0.9	94	86	68	32
1.0	96	89	73	37

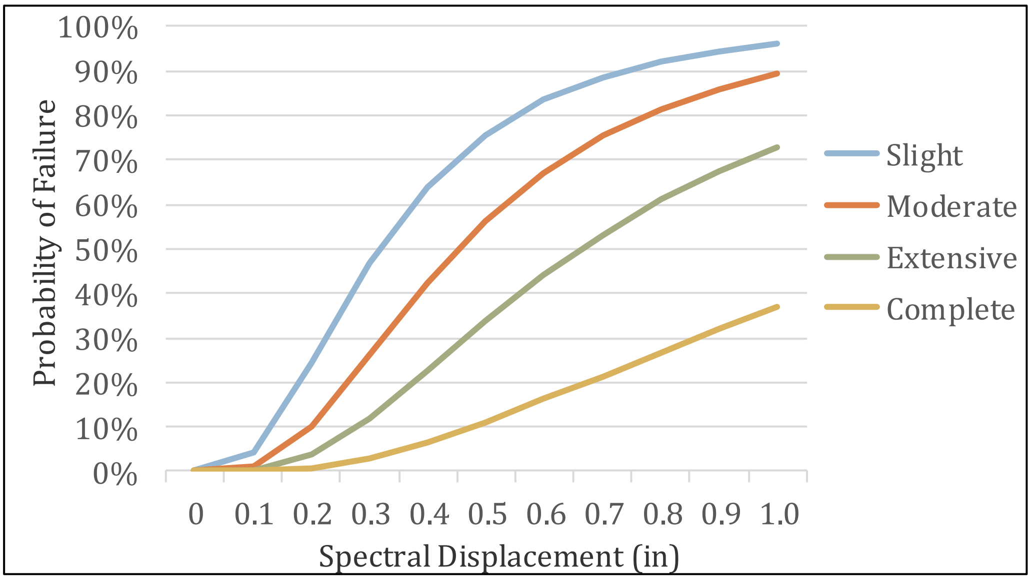

Figure 3. Fragility Curve for Bottom Mass Irregular Building (Push X direction)

Table 6. Probabilities of Failures for Bottom Mass Irregular Building (Push Y direction)

S_d (in)	Probability of Failures (%)			
	Slight	Moderate	Extensive	Complete
0	0	0	0	0
0.1	84	68	36	9
0.2	98	94	75	32
0.3	100	99	90	52
0.4	100	100	96	66
0.5	100	100	98	76
0.6	100	100	99	83
0.7	100	100	99	87
0.8	100	100	100	90
0.9	100	100	100	93
1.0	100	100	100	94

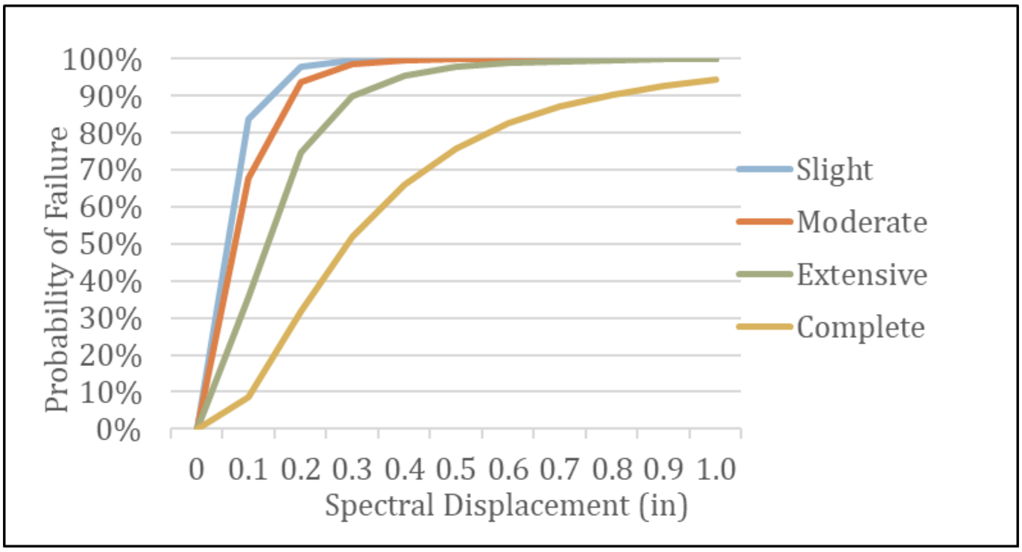

Figure 4. Fragility Curve for Bottom Mass Irregular Building (Push Y direction)

A comparison of fragility curves for different damage states in the push X and Y directions reveals a higher probability of failure in the push Y direction. A steeper curve in the Y direction for all damage states (slight, moderate, extensive, and collapse) suggests that not only is the structure more prone to early damage in the Y direction, but the progression of damage is also quicker. The building is likely to progress from minor to severe damage much more rapidly when subjected to seismic forces along the Y axis. This indicates greater structural vulnerability to seismic forces along the Y direction due to reduced lateral stiffness and strength, resulting in higher deformation demands and earlier structural failure. So, the building reaches higher damage states at lower seismic intensities when pushed in the Y direction, suggesting that the Y axis has lower resistance to lateral forces than X axis in this structure.

Table 7. Probabilities of Failures for Middle Mass Irregular Building (Push X direction)

S_d (in)	Probability of Failures (%)			
	Slight	Moderate	Extensive	Complete
0	0	0	0	0
0.1	1	0	0	0
0.2	8	2	1	0
0.3	21	8	4	1
0.4	36	17	9	3
0.5	49	28	16	5
0.6	60	38	23	9
0.7	68	48	31	12
0.8	75	56	38	16
0.9	81	63	45	20
1.0	85	69	51	24

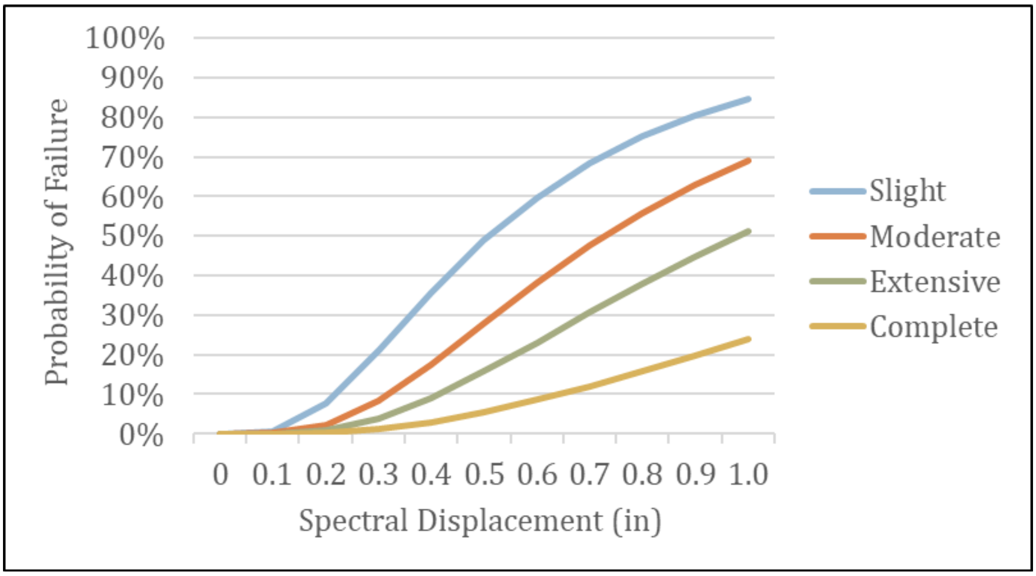

Figure 5. Fragility Curve for Middle Mass Irregular Building (Push X direction)

Table 8. Probabilities of Failures for Middle Mass Irregular Building (Push Y direction)

S_d (in)	Probability of Failures (%)			
	Slight	Moderate	Extensive	Complete
0	0	0	0	0
0.1	12	4	0	0
0.2	45	24	0	0
0.3	69	48	0	0
0.4	82	65	0	0
0.5	90	77	1	0
0.6	94	85	1	0
0.7	96	90	2	0
0.8	98	93	4	0
0.9	98	95	5	0
1.0	99	97	7	0

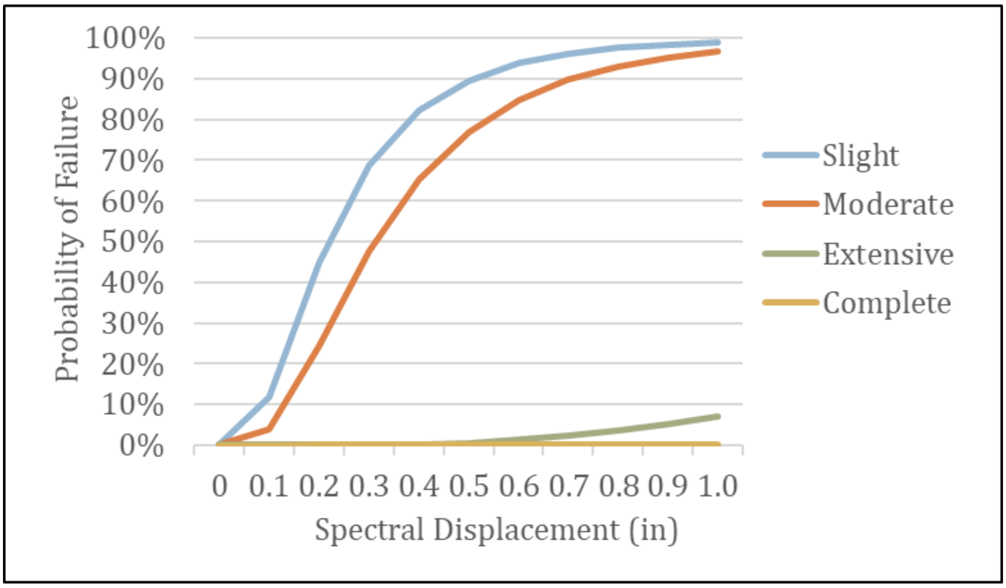

Figure 6. Fragility Curve for Middle Mass Irregular Building (Push Y direction)

Table 7 and Table 8 present the failure probabilities for the middle mass irregular building at different damage states. Fragility curves for middle mass irregular building for push X and Y direction are presented in Figure 5 and Figure 6, respectively. Comparing fragility curves for different damage states in the push X and Y directions shows a higher failure probability in the push Y direction. As seismic intensity increases, the probability of failure rises faster in this direction. The push Y direction likely has reduced structural capacity, which could be due to lower lateral stiffness, weaker reinforcement, or lesser ductility in the push Y direction compared to the push X direction. As a result, the building performs better in the X direction, suggesting that after yielding, it can continue deforming and absorbing energy, thereby delaying severe damage states like collapse.

Table 9. Probabilities of Failures for Top Mass Irregular Building (Push X direction)

S_d (in)	Probability of Failures (%)			
	Slight	**Moderate**	**Extensive**	**Complete**
0	0	0	0	0
0.1	0	0	0	0
0.2	3	1	0	0
0.3	11	3	2	1
0.4	21	8	4	1
0.5	32	15	8	3
0.6	43	23	13	5
0.7	52	31	19	7
0.8	60	38	24	10
0.9	67	46	30	12
1.0	72	52	36	15

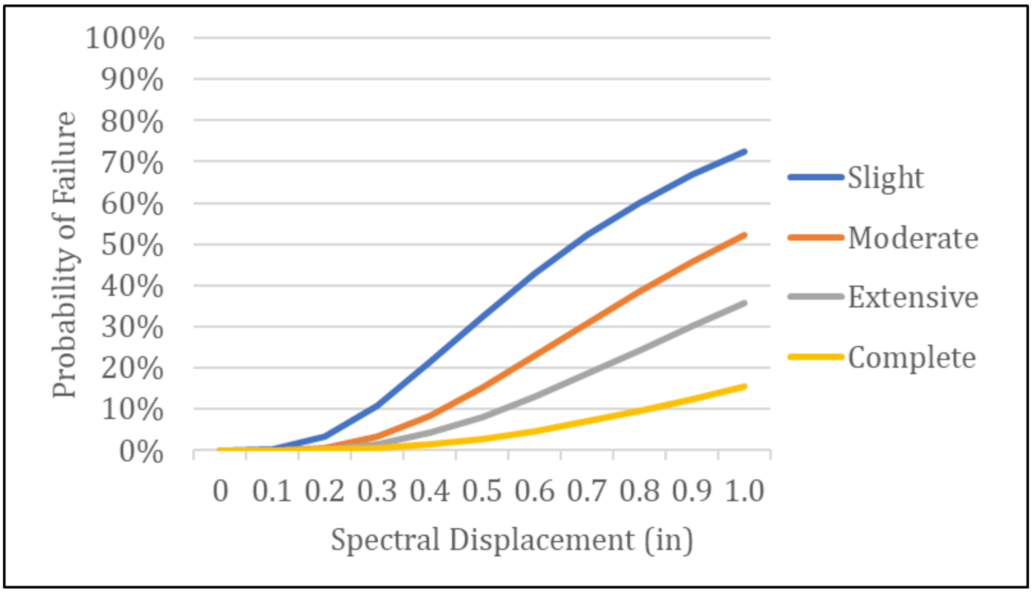

Figure 7. Fragility Curve for Top Mass Irregular Building (Push X direction)

Table 10. Probabilities of Failures for Top Mass Irregular Building (Push Y direction)

S_d (in)	**Probability of Failures (%)**			
	Slight	**Moderate**	**Extensive**	**Complete**
0	0	0	0	0
0.1	10	3	0	0
0.2	40	21	0	0
0.3	64	43	0	0
0.4	79	61	0	0
0.5	87	73	0	0
0.6	92	82	0	0
0.7	95	87	0	0
0.8	97	91	1	0
0.9	98	94	1	0
1.0	99	96	1	0

Table 9 and Table 10 show the failure probabilities of the top mass irregular building at different damage states for the push X and Y directions, respectively. The corresponding fragility curves are presented in Figure 7 and Figure 8. Comparing the failure probabilities for different damage states in the push X and Y directions shows a higher probability of failure in the push Y direction. However, in the push Y direction, failures are mainly observed in the slight and moderate damage states, while there is almost no failure in the extensive and complete damage states.

When analyzing the mass irregular effect in different locations in the same building, it was found that the probability of failure percentage was higher in the push Y directcion. So, the higher probability of failure in the Y direction highlights the structural weaknesses that make the building more susceptible to damage under seismic forces along this axis.

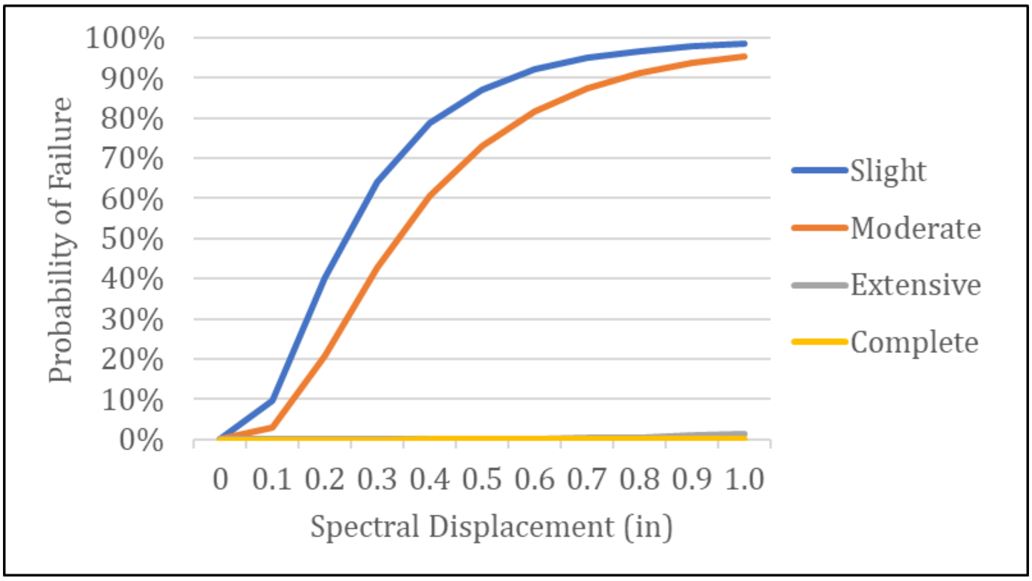

Figure 8. Fragility Curve for Top Mass Irregular Building (Push Y direction)

In this study, a building was analyzed considering three distinct locations of mass irregularity, with concrete having a compressive strength of 4000 psi and reinforcing bars possessing a yield strength of 50,000 psi. After performing the pushover analysis for these buildings, the plastic hinges for each story are counted to determine the building's performance level. The comparison of performance points for each mass irregular buildings with respect to the displacement and base shear for push X and Y direction are shown in Table 11 and Table 12, respectively.

Table 11. Comparison of Performance Points (Push X direction)

Irregularity Type	Displacement (in)	Base Shear (kip)	Performance Level
Bottom Mass-BMI	2.51	2857	IO-LS
Middle Mass-MMI	2.60	2217	B-IO
Top Mass-TMI	2.88	1867	CP-C

Table 12. Comparison of Performance Points (Push Y direction)

Irregularity Type	Displacement (in)	Base Shear (kip)	Performance Level
Bottom Mass-BMI	0.52	3164	IO-LS
Middle Mass-MMI	0.53	2362	B-IO
Top Mass-TMI	0.56	1947	CP-C

According to the summary results, the maximum displacement in the push-X direction was observed in the top mass irregular building, measuring 2.88 inches with a corresponding base shear of 1867 kips. Similarly, in the push-Y direction, the maximum displacement was recorded as 0.56 inches, with a corresponding base shear of 1947 kips.

The local vulnerability index values are evaluated based on the plastic hinge formation obtained from the pushover analysis. Calculating the index requires determining the number of plastic hinges formed in the frame elements at each performance level. The plastic hinges color change their states namely- Operational (B), Immediate occupancy (IO), Life safety (LS), Collapse prevention (CP), and Collapse (C). Using the color-coded display of plastic hinges, vulnerability is quantified according to Table 4 and equation (2), as explained earlier, with the results presented in Table 13.

Table 13. Vulnerability Index Results

Irregularity Type	Performance Range					Vulnerability Index Value (VI)
	B-IO	IO-LS	LS-CP	CP-C	Total	
BMI	10075	4	0	1	10080	0.71
MMI	10080	0	0	0	10080	0.00
TMI	10076	1	2	1	10080	0.94

From the vulnerability index obtained by the analysis, five vulnerability levels are proposed (Green 1, Green 2, Orange 3, Orange 4, Red 5) to evaluate the seismic performance of the buildings, this classification is illustrated in Table 14 [14].

Table 14. Vulnerability Classification According to VI Value [14]

Vulnerability Levels	Green		Orange		Red
	1	2	3	4	5
VI	0.10-0.20	0.20-0.40	0.40-0.55	0.55-0.70	0.70-1.00
$VI_{,mean}$	0.150	0.300	0.475	0.625	0.850

The vulnerability classifications were correlated with observed damage, described as; Negligible, Minor, Moderate, Severe (partial collapse), and Total Collapse as shown in Table 15[14].

Table 15. Vulnerability Categories According to the Observed Damage[14]

Damage Categories	Levels	Descriptions
Negligible	Green 1	Negligible to light damage
Minor	Green 2	Light for structural elements, and moderate for non-structural elements
Moderate	Orange 3	Moderate for structural elements, and heavy for non-structural elements
Severe	Orange 4	Heavy for both the structural and non-structural elements
Total Collapse	Red 5	Total failure or collapse of the structure

Based on the computed structural vulnerability index values, mass irregular buildings fall under vulnerability category level 5.

D. Conclusion

This study aimed to investigate the impact of mass irregularity on building performance and seismic vulnerability, represented by the structural vulnerability index (VI), for an existing reinforced concrete rectangular building in Mandalay. Based on the study analyzing the structural vulnerability of irregular frame buildings by plotting fragility curves and determining seismic vulnerability index based on hinge formation, the following conclusions were drawn:

a. The probability of failure in both the push-X and push-Y directions for all irregular models revealed a higher failure percentage in the push-Y direction. This suggests that the structure is more susceptible to seismic excitation in that direction.
b. It can be concluded through the development of plastic hinges, there is a reduction in stiffness at the lower portion of the structures.
c. Among all irregular models, the top mass irregular building was found to be more vulnerable in pushover analysis and the middle mass irregular building was found to be better performance than others.
d. The effect of mass irregularity, especially in irregular structures, significantly impacts seismic performance, particularly in the push-Y direction of top mass irregular buildings.

E. Acknowledgment

First of all, the author sincerely appreciates the support and encouragement of Dr. San Yu Khaing, Rector (Acting), Mandalay Technological University. The author is deeply indebted to Dr. Nilar Aye, Professor and Head of the Department of Civil Engineering at Mandalay Technological University, for her valuable suggestions and support throughout the completion of this study. The author also thanks all of the teachers from the Department of Civil Engineering, Mandalay Technological University, for their effective suggestions and help. Finally, the author is deeply grateful to her beloved parents for their support, advice and encouragement.

F. References

[1] W Arif and I G Craifaleanu, “Assessment of the Seismic Vulnerability of a Multi-story RC Structure with Plan Irregularity”, *IOP Conference Series*, Earth and Environmental Science, October, 2023.

[2] Ravikumar C M, Babu Narayan K S, Sujith B V and Venkat Reddy D, “Effect of Irregular Configurations on Seismic Vulnerability of RC Buildings,”, AR Architecture, Research. 2012/1. ISSN 1580-5573, ISSN 1581-6974, vol.2, Issue. 3: 20-26.

[3] Omar Nady, Sameh Youssef Mahfouz, and Salah El-Din Fahmy Taher, “Quantification of Vertical Irregularities for Earthquake Resistant Reinforced Concrete Buildings,” http://www.mdpi.com/journal/buildings, 12081160, vol. 12, Issue. 8, 19 pages, August 2022.

[4] “Myammar National Building Code”, MNBC 2020.

[5] American Society of Civil Engineers, “Minimum Design Loads for Buildings and other Structures”, ASCE/SEI 7-16.

[6] ETABS (2019) Version 19.0.0, Computer and Structure Institute.

[7] "HAZUS MH-MR4: Multi-hazard Loss Estimation Methodology": Technical Manual, Federal Emergency Agency, Washington, D.C, 2009.
[8] American Concrete Institute, "Building Code Requirements for Structural Concrete", (ACI 318-19).
[9] "Seismic Evaluation and Retrofit of Existing Building", ASCE/SEI 41-17.
[10] "Seismic Evaluation and Retrofit of Concrete Buildings. Applied Technology Council, 555. Twin Dolphin Drive, Suite 550 Redwood City, California, ATC-40, 1996.
[11] "Improvement of Nonlinear Static Seismic Analysis Procedures", FEMA440, June 2005.
[12] Lantada, N., Pujades, L.G., & Barbat, A. H. (2009)."Vulnerability index and capacity spectrum based methods for urban seismic risk evaluation. A comparison. *Natural Hazrads*, 51, 501-524.
[13] N.Lakshmanan, "Seismic Evaluation and Retrofitting of Buildings and Structures," *ISET Journal of Earthquake Technology*, vol. 43, no 1-2, pp. 31-48, March-June 2006.
[14] F.I. Belheouane, M. Bensaibi "Assessment of Vulnerability Curves using Vulnerability Index Method for Reinforced Concrete Structures", World Acad. Sci. Eng. Technol. Int. J. Civ. Archit. Sci. Eng. 7 : p. 153-156, 2013.